Lazaro et al

Supplement figure 1: Human PBMC cytosolic extracts used for peptide stability assays are devoid of lysosomal activities.

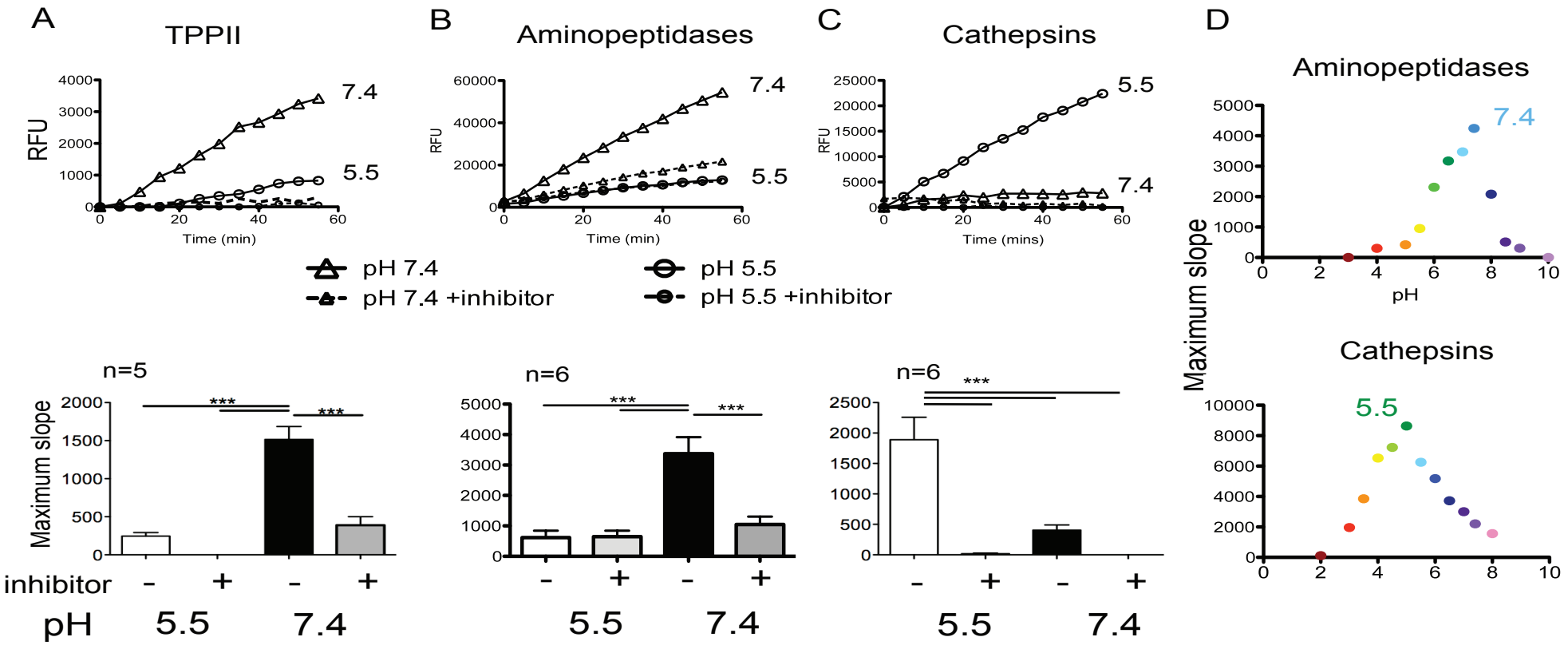

Supplementary figure 1: Human PBMC cytosolic extracts used for peptide stability assays are devoid of lysosomal activities.
A-C: Hydrolytic activities specific for several cytosolic peptidases (TPPII in panel A, aminopeptidases in panel B) or lysosomal cathepsins (panel C) were measured with peptidase-specific fluorogenic substrates in cytosolic extracts prepared at pH 7.4 (triangles) or in whole extracts prepared at pH 5.5 (circles) in the absence (plain lines) or presence (dotted lines) of specific inhibitors. Fluorescence emission after peptide cleavage is proportional to the activity. Specific inhibitors used on each panel were butabindide, bestatin and E64 to control the specific activities of TPPII, aminopeptidases and cathepsins respectively. The upper panels show peptidase activities measured every 5 minutes for one hour.
The lower panels show maximum slopes of these kinetics for extracts prepared from 5 to 6 healthy donors. Average of 5 or 6 experiments ± SD analyzed by one-way ANOVA with Bonferroni multiple comparison test.
D. Aminopeptidases (upper panel) and cathepsins (lower panel) activities were measured in whole extracts from the same donor prepared at pH ranging from 2 to 10. Representative of 3 donors.

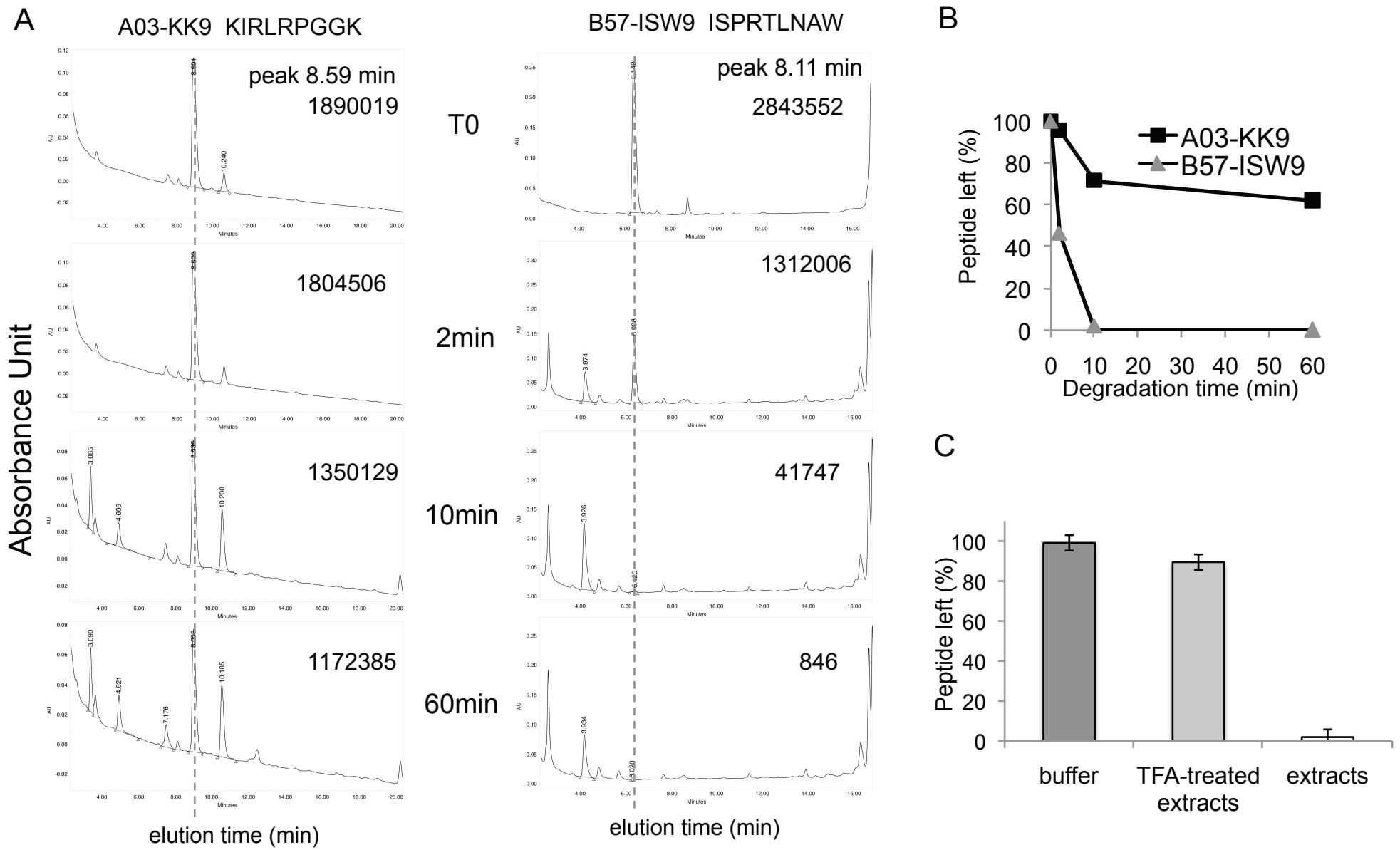

Supplementary figure 2: RP-HPLC profiles of peptides during cytosolic degradation.
A: Peptide A03-KK9 (left column) and B57-ISW9 (right column) were incubated in cytosolic extracts. Aliquots of equal amounts were taken after 0, 2, 10, 60 minutes and analyzed by RP-HPLC. A peptide is detected by measurement of absorbance at 280nm and identified by a peak at a defined elution time. The surface under peak is indicated in the upper right corner and is proportional to the amount of peptide for a given peptide. B. Quantification of A03-KK9 (black square) and B57-ISW9 (grey triangle) over time. 100% represent the peptide peak surface at time 0. Similar results were obtained with cytosol from several healthy donors with or without the HLA restricting the epitope, ruling out that variations in peptide stability were due to trapping by contaminant MHC-I molecules. C. Peptide recovery from extracts and detection by RP-HPLC: Different unstable peptides were incubated 10 minutes in buffer (dark grey bar), cytosolic extracts inactivated with TFA prior to peptide addition (light grey bars), or active cytosolic extracts (white bars). The amount of peptide left was analyzed by RP-HPLC; 100% is the peak surface at time 0 for each peptide incubated in buffer. Average of 3 experiments ± SD. Peptides incubated in buffer or in extracts pre-inactivated with TFA yielded similar HPLC peaks (less than 10% difference in peak surface), demonstrating efficient peptide recovery and that the reduction of peptide peak surface incubated with cytosol is therefore due to a cytosol-induced degradation.

Supplement figure 3: Different cytosolic stability of peptides affect epitope presentation and recognition by CTL

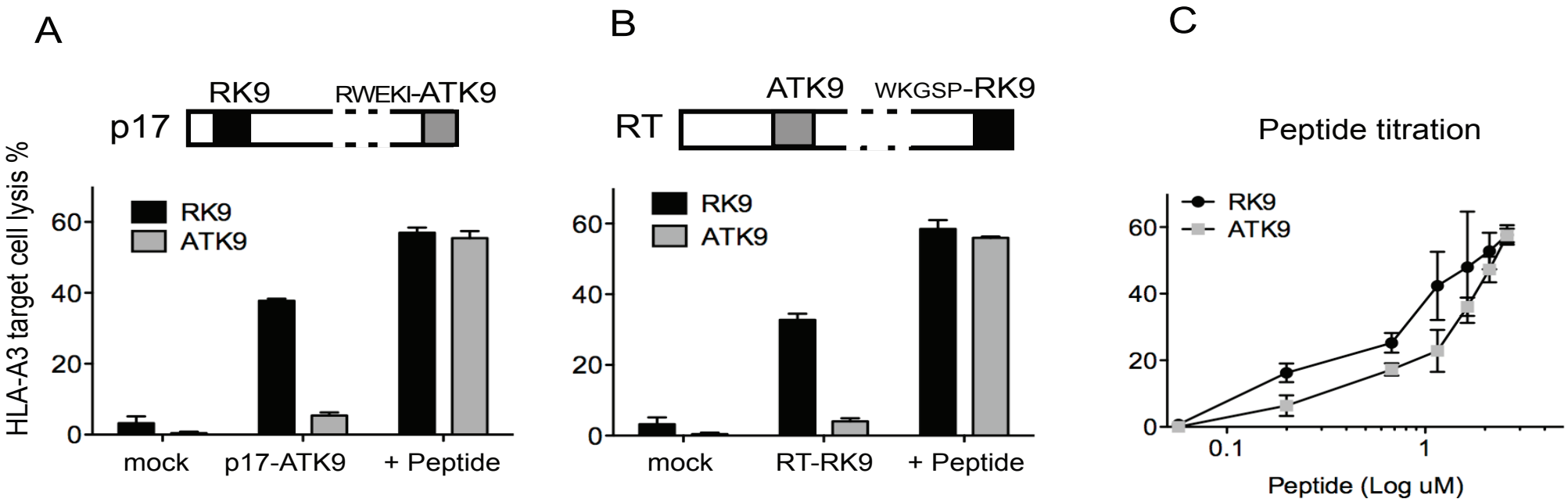

Supplementary figure 3: Differences in cytosolic stability of peptides affect epitope presentation and recognition by CTL.
A. HeLa-A03 cells (HeLa cells stably expressing HLA-A03) were transfected with a CMV-driven vector expressing HIV Gag p17 with RWEKI-ATK9 appended at the C-terminal end such that RK9 and ATK9 are flanked by the same N-flanking motif RWEKI. Mock- (left columns) or p17-RWEKI-ATK9-transfected cells (middle columns) were used as targets in a chromium cytolysis assay with RK9- (black bars) or ATK9-specific (grey bars) CTL. Positive controls include transfected cells with exogenously added peptides (right columns).
B. Similar to A except cells were transfected with CMV-RT-WKGSP-RK9.
C. RK9 and ATK9 peptide titration on HeLa-A03 cells. By comparing the lysis % of transfected cells to that of cells pulsed with increasing amounts of RK9 or ATK9, the equivalent amount of epitopes presented from cells expressing p17-RWEKI-ATK9 was 9.8uM for RK9 and 1.2uM for ATK9, and for cells expressing RT-WKGSP-RK9, 6.9uM RK9 and 1.3uM ATK9. A-C: Average of 3 experiments ± SD.

Lazaro et al supplementary figures

Supplementary figure 4: Predictive model for intracellular peptide stability and model validation

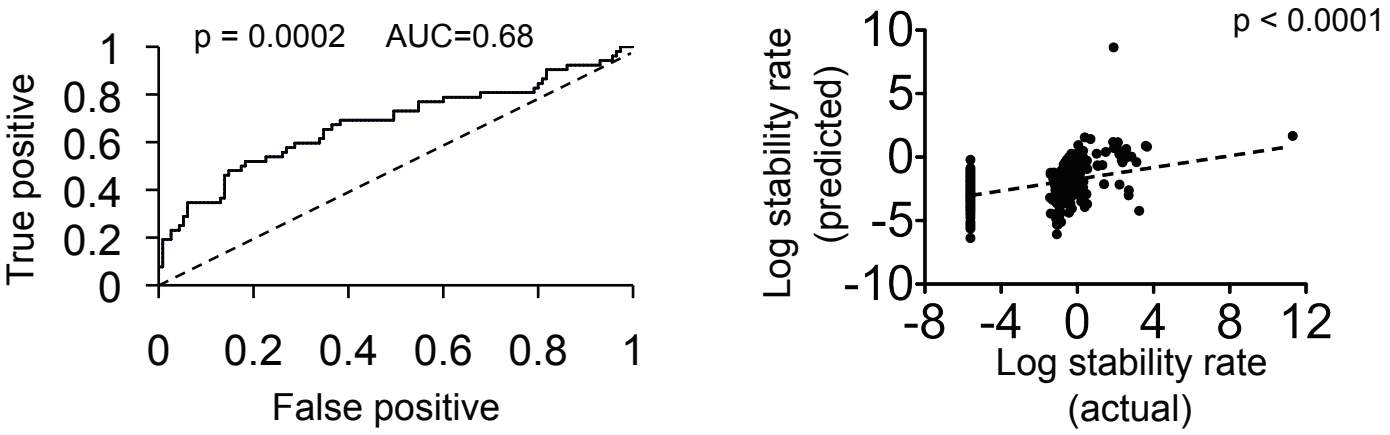

Supplementary figure 4: Predictive model for intracellular peptide stability and model validation
L1-regularized logistic regression (20) was used to predict intracellular peptide stability as this method has allowed the improvement of MHC-I epitope prediction (19). The model can be written

$$\log \frac{p(y \mid x_1, \ldots, x_m)}{1 - p(y \mid x_1, \ldots, x_m)} = w_0 + \sum_{i=1}^{m} w_i x_i$$

where y denotes whether the peptide is stable (y=1) or not (y=0), xi, i=1,…,m, are features describing aspects of the peptide (biochemical features of single or groups of amino acids), wi, i=0,…,m are weights, and p(y|x1,…,xm) is the probability that the peptide is stable given its features. The weights were estimated from the data, by finding the values of the weights that maximized the log likelihood of the data minus an L1 term that is proportional to the sum of the absolute value of the weights. In general, use of the L1 term drives many of the weights to zero and leads to better prediction (20). The proportionality factor in the L1 term was selected so as to maximize the out-of-sample log likelihood via 10-fold cross-validation. Features with less than three positive instances were removed prior to analysis.
http://research.microsoft.com/en-us/um/redmond/projects/MSCompBio/StabilityPrediction/.

Left: ROC curve of the stability rate prediction model measuring the proportion of true positive vs. false positive values (Area Under Curve AUC=0.68). The dotted diagonal illustrates random events distribution threshold.
Right: Correlation between the Log of stability rates determined experimentally (actual stability rates, x axis) and that of stability rates predicted by the model (predicted stability rates, y axis). p<0.0001.
Statistical analyses are performed with a Spearman test.

Supplementary figure 5: Stability and degradation of peptides are independent saturable mechanisms

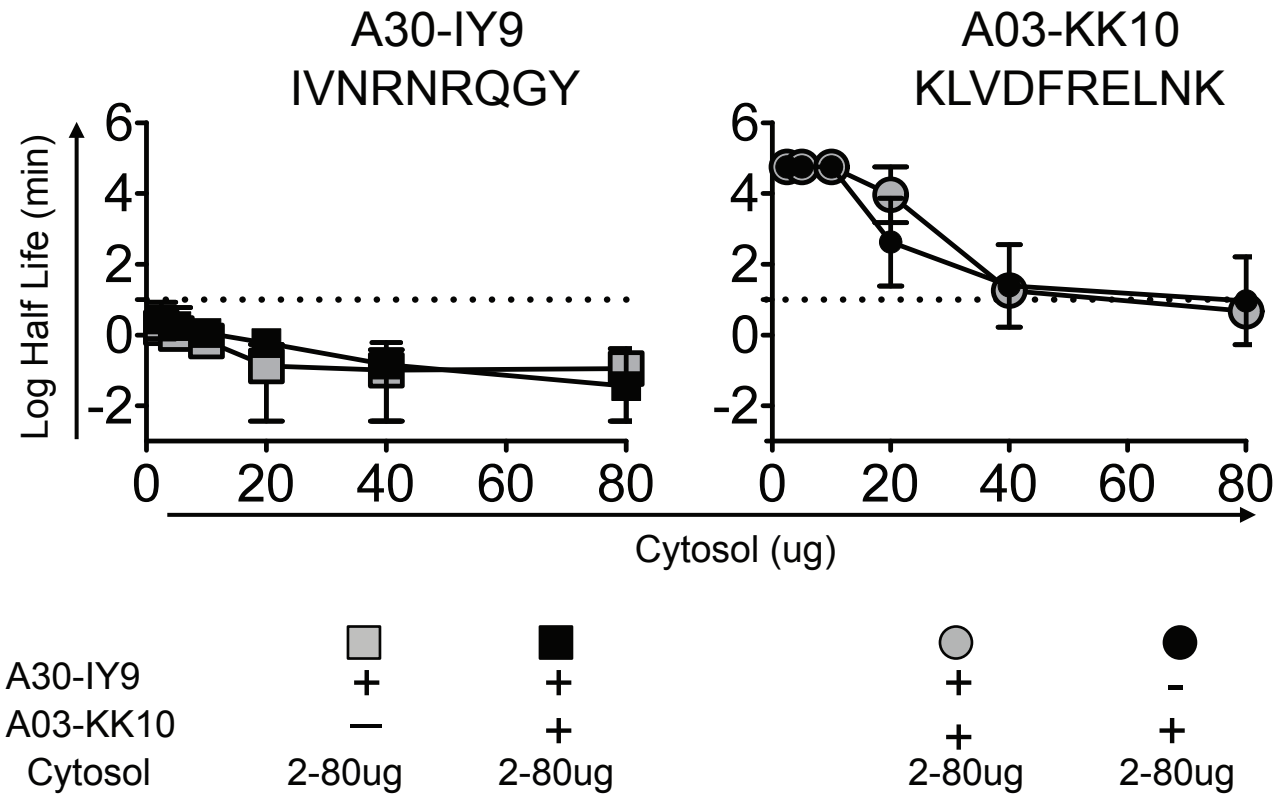

Supplementary figure 5: Stability and degradation of peptides are independent saturable mechanisms.
Left panel: Unstable HLA-A30 IY9 (IVNRNRQGY, aa 704-712 in gp160) (half-life 0.38min) was degraded for 30 minutes with increasing amounts of cytosol in the presence (black squares) or absence (grey squares) of stable HLA-A03 KK10 (KLVDFRELNK, residues 73-82 in RT, stability rate 14.9; half-life >90 minutes).
The Log stability rates of each peptide for each cytosol amount are indicated. IY9 was stable only when peptide was in large excess (at 2.5ug cytosol, IY9 stability rate 2.4; half-life 35 minutes), but the stability rate of this peptide decreased by 7.7-fold as the amount of cytosol was increased to 20ug, and was short (0.34 to 0.31; half-life 18 seconds) with >20ug cytosol.
Right panel: Stable peptide HLA-A03 KK10 was degraded in the presence or absence of unstable HLA-A30 IY9. This peptide remained extremely stable at all conditions tested (stability rate 7.8 in 80ug cytosol; half-life 65 minutes).
The stability rate of each peptide was largely unaffected by the presence or absence of the other peptide, as indicated by the grey and black symbols for each panel (80-110% of half-life without a second peptide).
Data represent the mean of 3 independent experiments ± SD.
Similar results were obtained with six pairs of stable and unstable epitopes, as well as in assays where the stable peptide was pre-incubated for 30 minutes rather than co-incubated with the unstable peptide (data not shown).

Supplementary figure 6. Efficiency of immunodepletion of cellular targets in PBMC cytosol

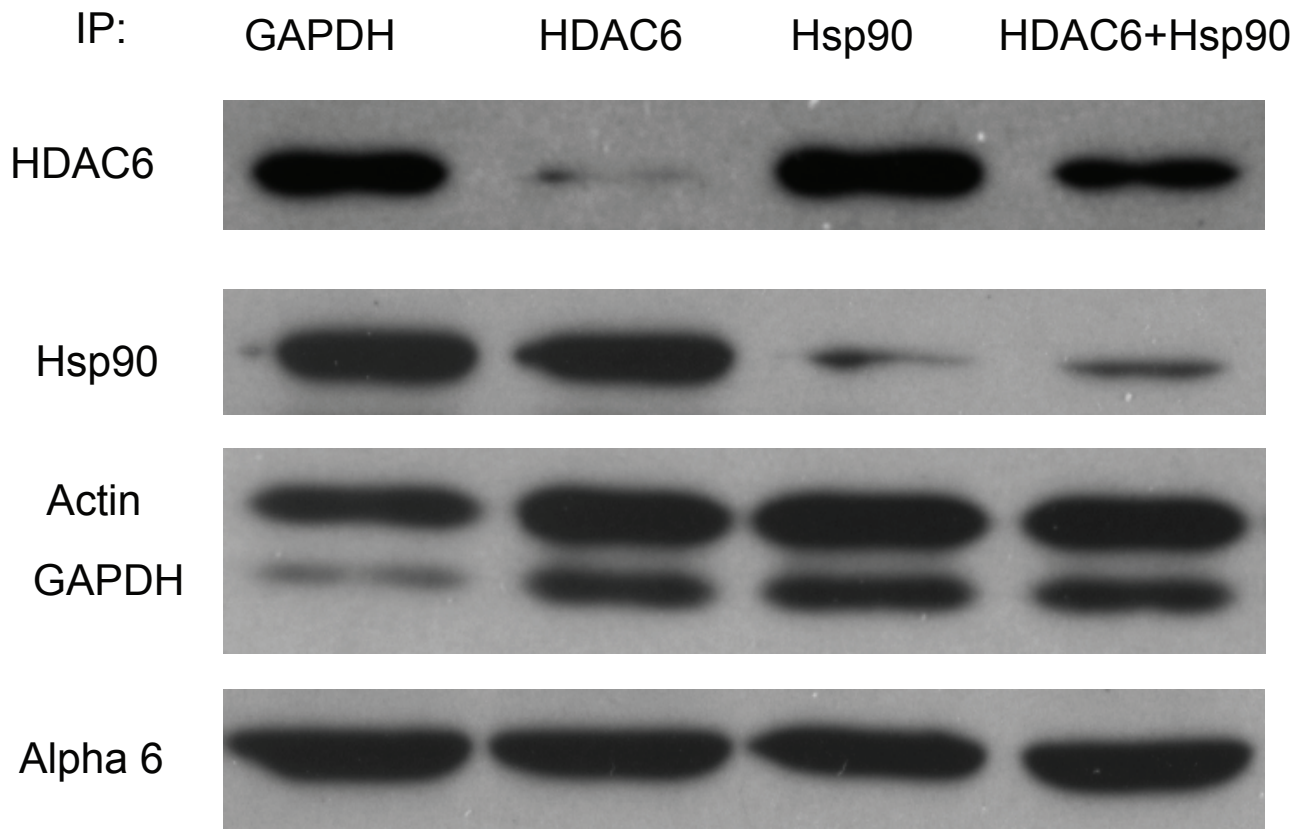

Supplementary figure 6. Efficiency of immunodepletion of cellular targets in PBMC cytosol.
PBMC cytosol was immunodepleted of Hsp90, HDAC6, Hsp90+HDAC6, GAPH or incubated with a species-matched control serum. Equal amounts of immunodepleted extracts were loaded onto a SDS page gel and the amount of Hsp90, HDAC6, GAPH and control actin were assessed by Western blot. Immunodepletion efficiency ranged between 70 to 95%.

Supplementary figure 7: An HLA-restricted mutation decreasing intracellular peptide half-life abolishes CTL recognition of HIV-infected cells

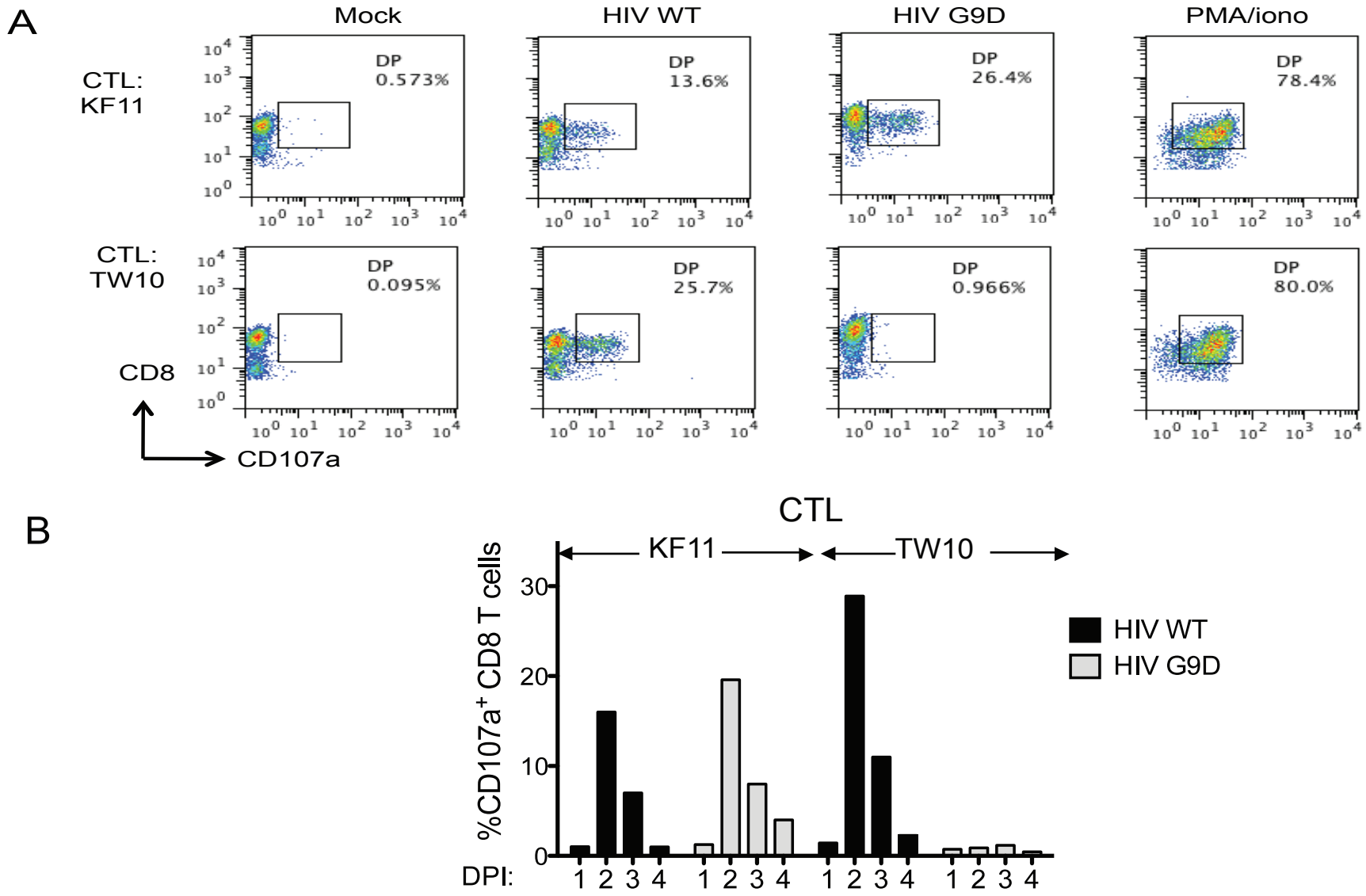

Supplementary figure 7: An HLA-restricted mutation decreasing intracellular peptide half-life abolishes CTL recognition of HIV-infected cells

A. B57-specific (top) or TW10-specific CTL (bottom) were mixed with HLA-B57 cells that had been mock-treated, infected with NL4-3 (HIV WT) or NL4-3 G9D (HIV G9D) 2 days before (left to right). Cells were stained for CD8 and CD107a and the % of double-positive cells (DP) was determined by FACS. PMA-ionomycin treatment of each CTL clone (right panels) is used as a positive control for CD107a degranulation.

B. Levels of CD8 and CD107a of KF11 (left) and TW10 CTL (right) were measured after incubation of each CTL with HLA-B57+ cells infected with HIV WT (black bars) or G9D (grey bars) at 1, 2, 3, 4 days post-infection (DPI).

Supplementary table 1: Amino acid features used for the computational identification of stability motifs

RESIDUES	AMINO ACID FEATURES											
	cyclic	aliphatic	aromatic	buried	hydrophobic	large	medium	small	negative	positive	charged	polar
ala A		*		*	*			*				
arg R						*				*	*	*
asn N							*					*
asp D							*		*		*	*
cys C				*			*					*
glu E						*			*		*	*
gln Q						*						*
gly G		*			*			*				
his H	*		*			*				*	*	*
ile I		*		*	*	*						
leu L		*		*	*	*						
lys K						*				*	*	*
met M				*	*	*						
phe F	*		*	*	*	*						
pro P	*				*		*					
ser S								*				*
thr T							*					*
trp W	*		*	*	*	*						
tyr Y	*		*		*	*						
val V		*		*	*		*					

Epitope name	Sequence	Stability rate
Cw3/Cw08-AL9 (Nef)	AALDLSHFL	0.003674
A1101-AK11 (p24)	ACQGVGGPGHK	0.003674
B45-AS10	AEAMSQVTNS	0.003674
B44-AW11 (p24)	AEQASQDVKNW	0.003674
B35-DL9 (gp120)	DPNPQEVVL	0.003674
B14-DA9 (p24)	DRFYKTLRA	0.003674
A6802-DWL9 (pro)	DTVLEEWNL	0.003674
B44-EW9 (pro)	EEMNLPGRW	0.003674
B8-EV9 (p17)	ELRSLYNTV	0.003674
B14-EL9 (gp41)	ERYLKDQQL	0.003674
A26-ER11(RT)	ETFYVDGAANR	0.003674
A26-EL9 (p24)	EVIPMFSAL	0.003674
A2-FK10 (p1)	FLGKIWPSYK	0.003674
Cw18-FF9 (p24)	FRDYVDRFF	0.003674
B18-FK10 (p24)	FRDYVDRFYK	0.003674
B57-FF9 (p24)	FSPEVIPMF	0.003674
B4002-GI9 (p15)	GELDRWEKI	0.003674
A3-GK9(RT)	GIPHPAGLK	0.003674
B1503/B72-GI9 (Pro)	GKKAIGTVL	0.003674
B1501-GY9(p24)	GLNKIVRMY	0.003674
B7-GL9 (p24)	GPGHKARVL	0.003674
A30-HY9 (gp120)	HIGPGRAFY	0.003674
A3-HK9 (Vif)	HMYISKKAK	0.003674
B1510-HL9 (p24)	HQAISPRTL	0.003674
B57-HW9 (nef)	HTQGYFPDW	0.003674
B4001-IL10 (p17)	IEIKDTKEAL	0.003674
A2-IV9 (RT)	ILKEPVHGV	0.003674
B14-IL8 (RT)	IRYQYNVL	0.003674
B57-IF9 (Vif)	ISKKAKGWF	0.003674
A28-IV9 (PRO)	ITLWQRPLV	0.003674
Cw8-IL9 (RT)	IVTDSQYAL	0.003674
A11-IK10 (RT)	IYQEPFKNLK	0.003674
Cw8-KL10 (Nef)	KAAVDLSHFL	0.003674
B57-KV8 (protease)	KAIGTVLV	0.003674
B58-KW11 (Env)	KAYETEVHNVW	0.003674
A30-KIY9 (RT)	KLNWASQIY	0.003674
B57-KF9(Int)	KTAVQMAVF	0.003674
A24-LY10 (gp120)	LFCASDAKAY	0.003674
A2-LI9 (Pro)	LVGPTPVNI	0.003674
B38-MW9 (gp120)	MHEDIISLW	0.003674
B18-NY10 (RT)	NETPGIRYQY	0.003674
B35-NQY9(RT)	NPDIVIYQY	0.003674
B35-NY9 (p17)	NSSKVSQNY	0.003674
A2-PL10 (nef)	PLTFGWCYKL	0.003674
A25-QW11 (p24)	QAISPRTLNAW	0.003674
A24-RL11cons (p24)	RDYVDRFYKTL	0.003674
A2-RI10 (gp120)	RGPGRAFVTI	0.003674
B1503-RY9 (INT)	RKAKIIRDY	0.003674
B52-RI8 (p24)	RMYSPTSI	0.003674
B42/B7-RL10 (Rev)	RPAEPVPLQL	0.003674
B7-RV9 (Nef)	RPMTYKAAV	0.003674
B7-RI10 (gp120)	RPNNNTRKSI	0.003674
B07-TM9 (Nef consB)	RPQVPLRPM	0.003674
B13-RI9 (Nef)	RQDILDLWI	0.003674
B7-RY10 (Nef)	RQDILDLWIY	0.003674
B8-RL9(gp41)	RQGLERALL	0.003674
B2703-RK10(p24)	RRWIQLGLQK	0.003674
A2301-RL9 (gp41)	RYLKDQQLL	0.003674
A24-RW8(nef)	RYPLTFGW	0.003674
B4001-SL9 (p24)	SEGATPQDL	0.003674
Cw4-SF9 (gp120)	SFNCGGEFF	0.003674
B7-SM9(RT)	SPAIFQSSM	0.003674
B7-SV9(p24)	SPRTLNAWV	0.003674
B51-TI8 (RT)	TAFTIPSI	0.003674
B35-TW9 (gp41)	TAVPWNASW	0.003674
B7-TL9(p24)	TPQDLNTML	0.003674

A2-VL9 (RT)	VIYQYMDDL	0.003674
A2-VL10 (nef)	VLEWRFDSRL	0.003674
B35-VL11(gp120)	VPVWKEATTTL	0.003674
B3801-WI9 (vif)	WHLGQGVSI	0.003674
B1503-WF9 (NEF)	WRFDSRLAF	0.003674
B18-YY9(nef)	YPLTFGWCY	0.003674
Cw0303-YL9 (p24)	YVDRFFKTL	0.003674
B51-II10 (vif)	IPLGDAKLII	0.2386
A33-TW9 (nef)	TRYPLTFGW	0.2488
A26-EY9 (RT)	ETKLGKAGY	0.2749
B57-KY10 (Rev)	KAVRLIKFLY	0.2833
B35-VY8 (nef)	VPLRPMTY	0.2901
B51-LI9 (gp160)	LPCRIKQII	0.2943
B53-EW10 (Tat)	EPVDPRLEPW	0.303
B1503-FGY10 (int)	FKRKGGIGGY	0.314
B53-QW9 (p24)	QASQEVKNW	0.3237
Cw05-AM12 (p24)	AEQASQEVKNWM	0.3258
A1-RY9 (gp41)	RRGWEVLKY	0.3317
A32-PW10(RT)	PIQKETWETW	0.3372
B58-TW10 C clade	TSTVEEQQIW	0.3381
A2-YL9 (p24)	YVDRFYKTL	0.3427
A11-PK8 (nef)	PLRPMTYK	0.3477
B57-KF11(p24)	KAFSPEVIPMF	0.3539
B2705-RI10 (nef)	RRQDILDLWI	0.3566
B57-IW9(p24)	ISPRTLNAW	0.3596
B18-LY10(Vif)	LADQLIHLHY	0.3634
A25-EW10(p24)	ETINEEAAEW	0.3641
B4001-KSL9(p15)	KELYPLTSL	0.3738
B57-KI8(p24)	KAFSPEVI	0.3868
A30-KQY9 (env)	KYCWNLLQY	0.3888
B53-TL9 (p24 HIV-2)	TPYDINQML	0.3938
B7-TM9(nef)	TPQVPLRPM	0.3941
B27-VL9 (Vpr)	VRHFPRIWL	0.4033
A29-SY9(gp160)	SFEPIPIHY	0.4079
B35-HY9 (RT)	HPDIVIYQY	0.41
B8-EI8 (p24)	EIYKRWII	0.4273
B1503-FSY10	FQTKGLGISY	0.4279
A11-AK10 (Int)	AVFIHNFKRK	0.4298
B2705-GY10(gp41)	GRRGWEALKY	0.4366
A30-IY9(env)	IVNRNRQGY	0.4376
B8-GK9 (p17)	GGKKKYKLK	0.4477
B13-GI9 (RT)	GQGQWTYQI	0.4479
B8-DL9(p24)	DCKTILKAL	0.4646
B7-IL9 (gp41)	IPRRIRQGL	0.4663
B58-IAW9 (RT)	IAMESIVIW	0.4778
B42-LI9 (Int)	LPPIVAKEI	0.4886
B7-FL9(vpr)	FPRIWLHGL	0.4972
B57-AW9 (Vpr)	AVRHFPRIW	0.4979
B13-RI9 (p2p6p1p7)	RQANFLGKI	0.4983
B57-ISW9 (RT)	IVLPEKDSW	0.5082
B35-WF9 (p17)	WASRELERF	0.5147
A2-AL9 Vpr)	AIIRILQQL	0.5198
A3-AK11 (RT)	ALVEICTEMEK	0.536
B4001-IL8 (RT)	IETVPVKL	0.5369
B7-FL9 (nef)	FPVTPQVPL	0.5409
B58-RY11 (p17)	RSLYNTVATLY	0.5535
A3-RK10 (VIF)	RIRTWKSLVK	0.554
A68-IL9 (gp41)	IVTRIVELL	0.5757
B4001-IL9 (RT)	IEELRQHLL	0.5947
B4002-AV9 (p24)	AEWDRVHPV	0.5968
B55-VT10 (gp120)	VPVWKEATTT	0.6465
B4001-KGL9 (nef)	KEKGGLEGL	0.6621
A2-SL9 (p17)	SLYNTVATL	0.672
Cw8/A2-GL9 (Nef C)	GAFDLSFFL	0.6975
B7-TL10 (nef)	TPGPGVRYPL	0.8359
B44-AY9(gp160)	AENLWVTVY	0.8655
A3-QK10 (nef)	QVPLRPMTYK	0.8839
A1-YT9 (nef)	YFPDWQNYT	0.898
A11-QKK9 (RT)	QIIEQLIKK	0.9054
B8-FL8(nef)	FLKEKGGL	0.9245
B2705-KK10 (p24)	KRWIILGLNK	0.9769
B62/B1501-RA9 (nef)	RMRRAEPAA	0.9779

A03/11-ATK9 (RT)	AIFQSSMTK	1.001
A11-SK9 (gp120)	SVITQACPK	1.045
A30-KY9 (int)	KIQNFRVYY	1.046
B57-YY9 (nef)	YTPGPGIRY	1.067
A03-QR9 (RT)	QIYPGIKVR	1.228
A33-ER8 (gp41)	EVAQRAYR	1.297
A0205-RA9 (gp41)	RIRQGLERA	1.302
B07-HI10 (vif)	HPRVSSEVHI	1.358
B08-GL9(RT)	GPKVKQWPL	1.361
B44-AY10 (gp120)	AENLWVTVYY	1.365
A03-RY10 (p17)	RLRPGGKKKY	1.488
A33-VR10 (gp41)	VFAVLSIVNR	1.49
B13-GI11 (p24)	GQMREPRGSDI	1.622
A2902-LY9 (p17)	LYNTVATLY	1.697
B8-RL9 (gp120)	RVKEKYQHL	2.01
B57-TW10 (p24)	TSTLQEQIGW	2.232
A3-KK9 (p17)	KIRLRPGGK	2.899
B7-FR10(nef)	FPVTPQVPLR	2.951
A3-KK11 (Vif)	KTKPPLPSVKK	4.065
B2705-IK9(p17)	IRLRPGGKK	6.595
Cw0801-RM9 (gp160)	RAIEAQQHM	6.694
B35-NIY9 (p24)	NPVPVGNIY	10.71
A03-RK9 (p17)	RLRPGGKKK	12.93
A03-RK11 (RT)	RMRGAHTNDVK	14.81
A03-KK10 (RT)	KLVDFRELNK	14.91
B07-HA9 (p24)	HPVHAGPIA	25.83
B35-PY9 (p24)	PPIPVGDIY	39.09

Supplementary table 2: Cytosolic stability of all HIV WT peptides
From left to right: peptide name (HIV protein), sequence, peptide cytosolic stability. The stability rate is calculated as a non-linear regression (one-phase exponential decay) of the degradation profile over 30 minutes for an average of 3 to 5 degradation experiments with different donors, and confirmed with up to 12 different donors for the most stable epitopes. The stability rates correspond to actual half-lives of peptides of <10 sec (stability rate <0.01), 10-30sec (stability rate <0.5), 30-60sec (stability rate 0.5-1), 1-2 minutes (stability rate 1-2), >2 minutes for stability rate >2 (with half-life >75 minutes for the most stable peptide).